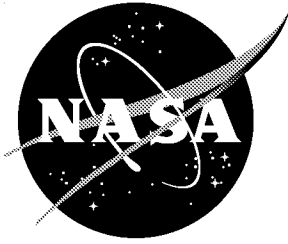


NASA/CR-2001-211255



Binaural Simulation Experiments in the NASA Langley Structural Acoustics Loads and Transmission Facility

Ferdinand W. Grosveld

Lockheed Martin Engineering and Sciences, Hampton, Virginia

December 2001

The NASA STI Program Office ... in Profile

Since its founding, NASA has been dedicated to the advancement of aeronautics and space science. The NASA Scientific and Technical Information (STI) Program Office plays a key part in helping NASA maintain this important role.

The NASA STI Program Office is operated by Langley Research Center, the lead center for NASA's scientific and technical information. The NASA STI Program Office provides access to the NASA STI Database, the largest collection of aeronautical and space science STI in the world. The Program Office is also NASA's institutional mechanism for disseminating the results of its research and development activities. These results are published by NASA in the NASA STI Report Series, which includes the following report types:

- **TECHNICAL PUBLICATION.** Reports of completed research or a major significant phase of research that present the results of NASA programs and include extensive data or theoretical analysis. Includes compilations of significant scientific and technical data and information deemed to be of continuing reference value. NASA counterpart of peer-reviewed formal professional papers, but having less stringent limitations on manuscript length and extent of graphic presentations.
- **TECHNICAL MEMORANDUM.** Scientific and technical findings that are preliminary or of specialized interest, e.g., quick release reports, working papers, and bibliographies that contain minimal annotation. Does not contain extensive analysis.
- **CONTRACTOR REPORT.** Scientific and technical findings by NASA-sponsored contractors and grantees.

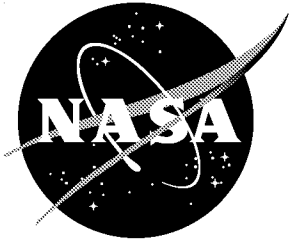
- **CONFERENCE PUBLICATION.** Collected papers from scientific and technical conferences, symposia, seminars, or other meetings sponsored or co-sponsored by NASA.
- **SPECIAL PUBLICATION.** Scientific, technical, or historical information from NASA programs, projects, and missions, often concerned with subjects having substantial public interest.
- **TECHNICAL TRANSLATION.** English-language translations of foreign scientific and technical material pertinent to NASA's mission.

Specialized services that complement the STI Program Office's diverse offerings include creating custom thesauri, building customized databases, organizing and publishing research results ... even providing videos.

For more information about the NASA STI Program Office, see the following:

- Access the NASA STI Program Home Page at **<http://www.sti.nasa.gov>**
- E-mail your question via the Internet to help@sti.nasa.gov
- Fax your question to the NASA STI Help Desk at (301) 621-0134
- Phone the NASA STI Help Desk at (301) 621-0390
- Write to:
NASA STI Help Desk
NASA Center for AeroSpace Information
7121 Standard Drive
Hanover, MD 21076-1320

NASA/CR-2001-211255



Binaural Simulation Experiments in the NASA Langley Structural Acoustics Loads and Transmission Facility

Ferdinand W. Grosveld

Lockheed Martin Engineering and Sciences, Hampton, Virginia

National Aeronautics and
Space Administration

Langley Research Center
Hampton, Virginia 23681-2199

Prepared for Langley Research Center
under Contract NAS1-00135

December 2001

Available from:

NASA Center for AeroSpace Information (CASI)
7121 Standard Drive
Hanover, MD 21076-1320
(301) 621-0390

National Technical Information Service (NTIS)
5285 Port Royal Road
Springfield, VA 22161-2171
(703) 605-6000

Introduction

Binaural simulation is the representation of sound as heard through the left and right ears of a listener and includes interaural signal time and intensity differences and the acoustic scattering about the head, pinnae and torso. The temporal differences occur naturally when a sound reaches the ears from one specific direction and may be measured by placing small microphones in the ears of a replica of a human head and torso. The relation between the two signals is preserved throughout the data acquisition and analysis process. The ambisonic B-format representation of sounds, including direction, consists of four signals. These signals represent the zero and first order spherical harmonics in three dimensions. The zero order harmonic (denoted W) is a sphere with an amplitude that is independent of direction. The three first order harmonics consist of dipoles in three mutually orthogonal directions. These are front-back (X), left-right (Y) and up-down (Z). The basic B-format representation of a reference and three vectors is mathematically simple to produce and is easily transcoded into other formats. Binaural simulation studies of sound radiating from structures are being pursued by the Virginia Polytechnic Institute and State University and NASA Langley Research Center under NASA cooperative agreement NCC-1-01029, "Development of an Efficient Binaural Simulation for the Analysis of Structural Acoustic Data." The purpose of the current work is to report on a matrix of binaural simulation measurements in a controlled acoustic environment to assist in the validation of these studies.

Test Facility

The measurements were conducted in the NASA Langley Research Center Structural Acoustic Loads and Transmission (SALT) facility. The arrangement of the anechoic chamber, the transmission loss (TL) window and the reverberation chamber is depicted in Figure 1. The anechoic chamber measures 4.57-m high, 7.65-m wide and 9.63-m long, measured from wedge tip to wedge tip for a volume of 337 m³. More than 4850 open-cell, polyether-polyurethane acoustic wedges cover the walls, the ceiling and the floor in the anechoic chamber. The movable partition (Figure 1) in front of the TL window was removed to accommodate the binaural simulation measurements. A 4.9-mm thick aluminum test panel, with an exposed area of 1.415- by 1.415-m, was installed in the TL window. Four 12.7-mm thick steel bars along the four edges of the panel provided an even distribution of the clamping forces applied to 56 bolts evenly spaced along the perimeter. The 278-m³ reverberation chamber is structurally isolated from the rest of the building and measures approximately 4.5 m by 6.5 m by 9.5 m. A cross-sectional view of the anechoic chamber showing the transmission loss window is presented in Figure 2. More detailed information on the SALT facility is provided in Reference 1. A location and positioning system was developed and implemented in the anechoic chamber of the SALT to accurately determine the coordinates of points in three-dimensional space. The method uses four reflective ball bearings, mounted onto the frame of the transmission loss window, as fixed reference points. The four reference points are in a plane parallel to the window frame. The system was extended to include reference points on the vertical side rail of the existing traverse system and the frame of the SALT facility entrance door. A trilateration procedure was formulated to calculate the coordinates for any specified location from the non-redundant distances to three calibrated reference points. A laser distance meter and a self-leveling laser vector alignment instrument were used for the distance measurements. Accuracy of the calculated coordinates, based on the measured distances, was within four millimeters.

Binaural Simulation Experiments

Measurements were made of the excitation, dynamic response and radiated sound field from the aluminum panel mounted in the transmission loss window of the SALT facility. Three basic sets of measurements were acquired in the anechoic room with and without the presence of a hard wall reflective surface:

1. Transfer functions were measured between a shaker source at two different panel locations and the vibrational response distributed over the panel surface using a scanning laser vibrometer.
2. Transfer functions, auto spectra and coherences were acquired between a shaker source at two different panel locations and the radiated sound at a number of freestanding microphone, B-format microphone and mannequin locations and for several positions and orientations of the mannequin.
3. The excitation time histories, panel response time histories at five locations, and the radiated sound time histories for a reference, a freestanding microphone, a B-format and two mannequin microphones were measured for broadband random, and transient input sources.

The first set of tests included only structural measurements. During the second and third sets of measurements acoustic as well as structural data was acquired and processed. Instrumentation was set up, configured and calibrated. The instrumentation included a personal computer (PC) based sound source generator, a shaker and signal amplifier, a force transducer, four panel-mounted accelerometers, one reference accelerometer on the mounting frame, two microphones with signal conditioners and power supplies, a band-pass filter, the Polytec laser vibrometer, the KEMAR (Knowles Electronics Manikin for Acoustic Research) binaural recording mannequin with the two microphones and signal conditioners, a B-format microphone with four output channels and the Structural Dynamics Research Corporation (SDRC) I-DEAS test data analysis software using the Hewlett Packard (HP) VXI ADC data acquisition system. The structural and acoustic data acquisition and analysis equipment is listed in Table 1. The components of the Polytec scanning vibrometer data acquisition and display system are summarized in Table 2. The components of the SDRC/HP/National Instruments (NI) data acquisition and analysis system are listed in Table 3. Measurements using the freestanding and the B-format microphones were made at the same positions as those made using the mannequin to obtain directly comparable data. This makes it possible to compare monaural recordings from the freestanding microphone with binaural recordings from the mannequin and B-format microphones.

Structural transfer functions

The aluminum test panel mounted in the TL window as viewed from the reverberation chamber is shown in Figure 3. The panel was instrumented with a shaker and four accelerometers. The shaker included a force gauge and an acceleration transducer. One of the accelerometers was mounted on the frame to detect possible flanking. The set up is shown in Figure 4. The coordinates of the measurement locations on the panel are listed in Table 4. The positive X-axis points to the left, when facing the panel from the reverberation chamber, while the Y-axis points up. One shaker location was chosen in the center of the panel to excite the lower-order odd modes of the panel (panel location ploc.1). The shaker location closer to one of the corner boundaries (panel location ploc.2) was selected to excite as many modes as possible. A close up of the mini shaker attached to the panel at

location ploc.2 is presented in Figure 5. Figure 6 shows a close-up view of the three panel-mounted accelerometers. The Cartesian panel coordinate system is shown in Figure 7 as viewed from the anechoic chamber. The Z-axis is perpendicular to the panel and points into the anechoic chamber. The Polytec scanning laser vibrometer (Figure 8) was positioned in the chamber at a stand-off distance 3089 mm from the panel center. This distance was optimized for the vibrometer by choosing $n=15$ in the formula $14 + n*205$. The stand-off distance formula was supplied by the manufacturer. The vibrometer measured the two-dimensional distribution of the vibrational velocities over the panel surface. The highly reflective surface of the panel was treated with a very thin white film to diminish scattering of the laser beam and increase the accuracy of the laser vibrometer measurements. The location of the vibrometer in the anechoic chamber is depicted in Figure 9. A 23 by 23 mesh was generated in the Polytec software and superimposed on the Polytec video image of the panel as shown in Figure 10. The transfer functions between the shaker point force input and the velocity at 529 points on the panel grid were measured with the laser vibrometer for the two shaker locations (ploc.1 and ploc.2) and pseudo-random noise input to the shaker. Related files were designated with the names 'Binpseudo2loc1Scan' and 'Binpseudo2loc2Scan'. The measurements were repeated for chirp noise input to the shaker when attached to the center (location ploc.1) of the panel. Files associated with these measurements were named 'Binchirp2loc1Scan'. The velocity was measured by the vibrometer with a sensitivity of 25 mm/s /V and a maximum range of 10V. The sensitivity factor of the reference acceleration was 1 m/s² /V with a maximum of 1V. Angle correction was automatically applied by the Polytec system. Sample bitmap graphic files of the panel velocity grid, with the extension '.bmp', were archived on compact disk number 1 (Table 5). The binary data files, which were acquired in Polytec software format with extensions '.svd', were stored on compact disk 2 and are tabulated in Table 6. Other, non-essential, files were written to compact disks 3 and 4 but are not listed here. The binary Polytec data files were converted to universal file format and archived on compact disks 5-7 (Tables 7-9).

Acoustic and structural response experiments

Anechoic environment: The panel Cartesian coordinate system shown in Figure 7 was used to identify microphone locations in the anechoic chamber, including the reference microphone (ref.mic), the freestanding microphone (mic-1), the two microphones in the ears of the mannequin (manikin-left and manikin-right), and the four transducers in the B-format (W, X, Y and Z) microphone. The coordinates of the measurement locations (loc.1 through loc.7) are summarized in Table 10. Figure 11 shows the Knowles Electronics Manikin for Acoustic Research (KEMAR). The support structure of the acoustic mannequin depicted in Figure 12 was designed to allow a range of rotational and angular attitudes. The local coordinate system of the mannequin and the positive rotation directions are indicated in Figure 12. The rotation about the Y-axis (phi.1) was measured with a torso-mounted protractor. The angles of rotation about the X-axis (phi.2) and the Z-axis (phi.3) were measured with a laser inclinometer. Accuracy of the measured angles was within ± 0.1 degree. The test matrix for the binaural simulation measurements is presented in Table 11. The schedule included 43 test runs for several locations of the measuring microphones, various attitudes of the mannequin, two locations of the shaker excitation and three different shaker inputs including pulse, broadband random, and pseudo-random. Measurements were taken for the 0-4000 Hz frequency band. Time histories were acquired for pulse and broadband random input to the shaker (pulse and random files in Table 11). The broadband random input was low-pass filtered at 2000 Hz. Transfer functions, auto spectra and

coherence functions were acquired for the pseudo-random excitation (transfer files in Table 11). The pseudo-random excitation was the same input from the arbitrary function generator as used for the structural transfer function measurements with the Polytec laser vibrometer system. Special measurement conditions for the binaural tests are listed in Table 12. An additional gain of 20 dB was applied to the mannequin microphone output signals for test number 35 to increase the measured dynamic response. The pulse input signal was changed from 4 V to 10 V for tests 39-43 and the pseudo random time input signals were changed from 4 V to 10 V for tests 40-43 to increase the output response levels. An additional gain of 20 dB was applied to the Y and Z channels of the B-format microphone for tests 40 and 43. None of these additional gains were included in the sensitivity factors of the IDEAS software and must be applied as corrections to the stored data. The file names in Table 11 were chosen to reflect the test type, test number, microphone identification, mannequin attitude if applicable, microphone location, and the shaker location on the panel. The name r8f45-n45-011f2 in Table 11, for instance, indicates files with time histories for broadband random noise excitation (r), test number 8 (8), rotation of the mannequin 45 degrees about Y-axis and -45 degrees about the X-axis (f45-n45-0), placement of the mannequin at location loc.1 (11) in the anechoic chamber and mounting of the shaker at location ploc.2 (f2) on the panel. Each file stores the signals from as many as fourteen channels (when all are active) including the shaker force transducer channel, five accelerometer response channels and eight channels for the reference microphone, the main microphone, the mannequin (two channels) and the B-format microphone (four channels). The channel calibration settings are presented in Table 13. The microphones were calibrated before each data run and were all within ± 0.1 dB of the initial calibration values. The pressure reference microphone ref.mic was replaced by another pressure reference microphone after test number 35 and recalibrated. The related sensitivity factor was changed in IDEAS. A pressure microphone was used for the freestanding microphone, mic-1, in the first 35 tests to provide additional reference data. This pressure microphone was replaced by a free-field microphone for tests 36-43 to accommodate comparison with the mannequin microphones and the B-format microphone data at the same locations. The free-field microphone was calibrated and the sensitivity factor was adjusted in IDEAS (Table 13). The initial data acquisition sampling, trigger, window, averaging, filter and measurement conditions are tabulated in Table 14. Figure 13 shows the mannequin at location loc.1, parallel to the panel with its positive local Z-axis pointing to the panel center corresponding to the first test configuration in Table 11. The attitude of the mannequin for a combination of a 45-degree rotation about the Y-axis and a rotation of minus 45 degrees about the X-axis is depicted in Figure 14 and corresponds to test number 8 in Table 11.

Reflective panel installed: The tests were repeated after a 1473 mm by 1473 mm reflective panel was installed along the left vertical edge of the test panel and perpendicular to the test panel surface. The binaural simulation test matrix for the reflective panel is presented in Table 15. Figures 15, 16 and 17 show three attitudes of the mannequin at location loc.1 with the reflective panel installed. The mannequin was positioned parallel with the panel in Figure 15 (Test 1a in Table 15), rotated 150 degrees about the Y-axis in Figure 16 (Test 25a in Table 15), and rotated 45 degrees about the Z-axis in Figure 17 (Test 7a in Table 15). The actual rotation in Figure 17 was about an axis located 848 mm below and parallel with the Z-axis, which not only resulted in a rotation angle about the Z-axis but also in an X and Y translation. The B-format microphone at measurement location loc.1 is shown in Figure 18. The mannequin at measurement location loc.2 is depicted in Figure 19. The mannequin was rotated minus 32.3 degrees about the Y-axis pointing directly with its nose to the

center of the test panel. The mannequin was then rotated 30 degrees about the X-axis to create test configuration 34a. Figure 20 shows the B-format microphone at measurement location loc.1 with the mannequin in the foreground at location loc.2. The distance from location loc.3 to the test panel was too long relative to the dimensions of the reflective panel. The long distance prevented sound reflections from reaching the microphones at location loc.3 and therefore no measurements were conducted at that location. Four additional measurements were performed with the B-format microphone at location loc.1. The B-format microphone was positioned with its manufacturer logo facing the test panel and was rotated four times 90 degrees in clockwise direction (b.psi in Table 15) to investigate the effect of its orientation on the directionality of the output signals.

Data Storage: The I-DEAS program could not retrieve the records in the files p5f0-30-011f2.ati, p6f0-n30-011f2.ati, p39bml21f2input10v.ati, r5f0-30-011f2.ati and r41bml43f2input10v.ati. These tests were set up again consistent with the original configuration and the data acquisition was repeated. The tests requiring the B-format microphone were not repeated, as the B-format microphone was no longer available. All the binary files were converted to the universal file format and were archived, along with the original files, onto thirteen compact disks. All files on each disk were compressed into one ZIP format file. The compressed ZIP files are available for download at the Universal Resource Locator (URL) <http://stab.larc.nasa.gov/PubData>. The compact disk numbers, the storage space on each disk required for the original files, the compressed file sizes and the file names are listed in Tables 5-9 and 16-21. Non-pertinent files were omitted from the database.

Summary

A location and positioning system was developed and implemented in the anechoic chamber of the SALT facility to accurately determine the coordinates of points in three-dimensional space. Transfer functions were measured between a shaker source at two different panel locations and the vibrational response distributed over the panel surface using a scanning laser vibrometer. The binaural simulation test matrix included test runs for several locations of the measuring microphones, various attitudes of the mannequin, two locations of the shaker excitation and three different shaker inputs including pulse, broadband random, and pseudo-random. Transfer functions, auto spectra and coherence functions were acquired for the pseudo-random excitation. Time histories were acquired for the pulse and broadband random noise input to the shaker. The tests were repeated with a reflective surface installed. Binary data files were converted to universal format and archived on compact disk.

Acknowledgements

The outstanding test support from Mr. Carlton Pike, Mr. Jay Moen and Mr. Bob Baals of the Gas, Fluids and Acoustics Research Support Branch at the NASA Langley Research Center is gratefully acknowledged. Discussions with Ms. Sherilyn Brown, Ms. Brenda Sullivan and Dr. Stephen Rizzi of the Structural Acoustics Branch are appreciated. The author wishes to acknowledge Mr. Brad Lunde, President of SoundField USA/TransAmerica Audio, Las Vegas, NV for providing the B-format microphone system. This work was supported by the NASA Langley Research Center, SAMS (NAS1-00135) PBC, Dr. Richard Silcox, Technical Monitor. Funding was provided by the Life Cycle Simulation element of the Intelligent Synthesis Environment Program under the task entitled "Structural Acoustic Simulation in Operational Environments." Dr. Stephen Rizzi, Task Lead.

Reference

1. Grosveld, Ferdinand W., "Calibration of the Structural Acoustic Loads and Transmission (SALT) Facility at NASA Langley Research Center," INTER-NOISE 99, International Congress on Noise Control Engineering, Fort Lauderdale, Florida, December 6-8, 1999.

Tables

Table 1. Structural and acoustic data acquisition and analysis equipment

1.	Bruel & Kjaer Power Amplifier 2706
2.	PCB Piezotronics 482A16 Signal Conditioner/Power supply
3.	PCB 4-channel ICP Sensor Signal Conditioner/AC Power Supply 44A101
4.	Bruel & Kjaer Mini Shaker Type 4810
5.	PCB Piezotronics Shaker Force/Acceleration Transducer 288D01
6.	Endevco Isotron PE Accelerometer Model 2250A-10
7.	Krohn-Hite Model 3342R Band Pass Filter
8.	Ithaco Amplifier Model 455/Power Supply Model P14
9.	Larsen Davis Model 812 Type I Integrating Sound Level Meter
10.	Bruel & Kjaer Two-channel Microphone Power Supply
11.	Bruel & Kjaer Free-field Microphone Type 4165
12.	Bruel & Kjaer Pressure Microphone Type 4134
13.	General Radio Type 1562-A Sound Level Calibrator
14.	GenRad 1986 Omnicol Sound Level Calibrator
15.	Polytec Scanning Vibrometer Data Acquisition and Display System
16.	SDRC I-DEAS/Hewlett Packard/National Instruments Data Acquisition & Analysis System
17.	Knowles Electronics Manikin for Acoustic Research (KEMAR) Mannequin
18.	SoundField ST250 Microphone System

Table 2. Components of the Polytec scanning vibrometer data acquisition and display system

1.	Polytec Scanning Vibrometer PSV 300
2.	Controller OFV-3001S
3.	Scanning Head OFV-056
4.	Polytec Junction Box PSV-Z-040
5.	Prema Arbitrary Function Generator ARB 1000
6.	Windows NT 4.0 Workstation, Pentium III – 700 MHz – 128 MB RAM
7.	Polytec GmHB Scanning Vibrometer Software Version 7.1
8.	Plexwriter 12/4/32 CD-R

Table 3. Components of the SDRC/HP/NI data acquisition and analysis system

1.	Hewlett Packard E1421B Mainframe
2.	Agilent 16-channel E1432A Front-end Module
3.	National Instruments VXI-MXI-2 Plug & Play Interface Card
4.	Windows NT 4.0 Workstation, Pentium III – 868 MHz – 256 MB RAM
5.	SDRC I-DEAS Software Version 8 with OpenGL Graphics Driver
6.	Hewlett Packard Laserjet Printer 4

Table 4. Coordinates of measurement locations on aluminum test panel

Panel location	Transducer	X-coordinate [mm]	Y-coordinate [mm]	Z-coordinate [mm]
ploc.1	force/accelerometer	0	0	0
ploc.2	accelerometer/force	-502	-500	0
ploc.3	accelerometer	-353	0	0
ploc.4	accelerometer	-712	0	0
ploc.5	accelerometer	-118	118	0

Table 5. Files archived on compact disk 1

Compact Disk 1: 4.5 MB (Compressed ZIP file: 302 KB)		
Binpseudo2loc1Scan.bmp	Binpseudo2loc2Scan.bmp	Binchirp2loc1Scan.bmp

Table 6. Files archived on compact disk 2

Compact Disk 2: 478 MB (Compressed ZIP file: 431 MB)		
Binpseudo2loc1Scan.svd	Binpseudo2loc2Scan.svd	Binchirp2loc1Scan.svd

Table 7. File archived on compact disk 5

Compact Disk 5: 640 MB (ZIP file: 207 MB)
Binpseudo2loc1Scan.unv

Table 8. File archived on compact disk 6

Compact Disk 6: 640 MB (ZIP file: 208 MB)
Bin pseudo2loc2Scan.unv

Table 9. File archived on compact disk 7

Compact Disk 7: 640 MB (ZIP file: 206 MB)
Binchirp2loc1Scan.unv

Table 10. Coordinates of measurement locations in the anechoic room of the SALT facility

Location	Transducer	X-coordinate [mm]	Y-coordinate [mm]	Z-coordinate [mm]
Loc.1	mannequin/mic-1/B-format mic	0	0	925
Loc.2	mannequin/mic-1/B-format mic	-1234	0	1953
Loc.3	mannequin/mic-1/B-format mic	0	0	3048
Loc.4	mannequin/mic-1/B-format mic	0	0	3229
Loc.5	reference microphone (ref.mic)	-1526	524	1147
Loc.6	microphone 1 (mic-1)	-1390	0	3270
Loc.7	reference microphone (ref.mic)	0	524	3196

Table 11. Binaural test matrix for measurements in the anechoic room of the SALT facility

BINAURAL TEST MATRIX IN THE ANECHOIC ROOM OF THE SALT FACILITY													
	<---- anechoic chamber locations ---->						shaker	<--- mannequin --->			file names		
test	loc.1	loc.2	loc.3	loc.4	loc.5	loc.6	ploc.	phi.1	phi.2	phi.3	pulse (.ati)	random (.ati)	transfer (.afu)
1	manikin				ref.mic	mic-1	2	0	0	0	p1f0-0-01f2	r1f0-0-01f2	t1f0-0-01f2
2	manikin				ref.mic	mic-1	2	30	0	0	p2f0-30-01f2	r2f0-30-01f2	t2f0-30-01f2
3	manikin				ref.mic	mic-1	2	90	0	0	p3f0-90-01f2	r3f0-90-01f2	t3f0-90-01f2
4	manikin				ref.mic	mic-1	2	150	0	0	p4f0-150-01f2	r4f0-150-01f2	t4f0-150-01f2
5	manikin				ref.mic	mic-1	2	0	30	0	p5f0-30-01f2	r5f0-30-01f2	t5f0-30-01f2
6	manikin				ref.mic	mic-1	2	0	-30	0	p6f0-n30-01f2	r6f0-n30-01f2	t6f0-n30-01f2
7	manikin				ref.mic	mic-1	2	0	0	45	p7f0-0-45f2	r7f0-0-45f2	t7f0-0-45f2
8	manikin				ref.mic	mic-1	2	45	-45	0	p8f45-n45-01f2	r8f45-n45-01f2	t8f45-n45-01f2
9	manikin				ref.mic	mic-1	2	-30	0	0	p9fn30-0-01f2	r9fn30-0-01f2	t9fn30-0-01f2
10	manikin				ref.mic	mic-1	2	-115	20	0	p10fn115-20-01f2	r10fn115-20-01f2	t10fn115-20-01f2
11	manikin				ref.mic	mic-1	2	-45	0	0	p11fn45-0-01f2	r11fn45-0-01f2	t11fn45-0-01f2
12	manikin				ref.mic	mic-1	2	45	-40	0	p12f45-n40-01f2	r12f45-n40-01f2	t12f45-n40-01f2
13	manikin				ref.mic	mic-1	2	0	-80	0	p13f0-n80-01f2	r13f0-n80-01f2	t13f0-n80-01f2
14	manikin				ref.mic	mic-1	2	180	0	0	p14f180-0-01f2	r14f180-0-01f2	t14f180-0-01f2
15	manikin				ref.mic	mic-1	2	-90	0	0	p15fn90-0-01f2	r15fn90-0-01f2	t15fn90-0-01f2
16	manikin				ref.mic	mic-1	2	-150	0	0	p16fn150-0-01f2	r16fn150-0-01f2	t16fn150-0-01f2
17	manikin				ref.mic	mic-1	2	45	0	0	p17f45-0-01f2	r17f45-0-01f2	t17f45-0-01f2
18	manikin				ref.mic	mic-1	2	-115	-20	0	p18fn115-n20-01f2	r18fn115-n20-01f2	t18fn115-n20
19	manikin				ref.mic	mic-1	2	45	20	0	p19f45-20-01f2	r19f45-20-01f2	t19f45-20-01f2
20	manikin				ref.mic	mic-1	2	45	-20	0	p20f45-n20-01f2	r20f45-n20-01f2	t20f45-n20-01f2
21	manikin				ref.mic	mic-1	1	0	0	0	p21f0-0-01f1	r21f0-0-01f1	t21f0-0-01f1
22	manikin				ref.mic	mic-1	1	0	30	0	p22f0-30-01f1	r22f0-30-01f1	t22f0-30-01f1
23	manikin				ref.mic	mic-1	1	30	0	0	p23f30-0-01f1	r23f30-0-01f1	t23f30-0-01f1
24	manikin				ref.mic	mic-1	1	90	0	0	p24f90-0-01f1	r24f90-0-01f1	t24f90-0-01f1
25	manikin				ref.mic	mic-1	1	150	0	0	p25f150-0-01f1	r25f150-0-01f1	t25f150-0-01f1
26	manikin				ref.mic	mic-1	1	0	-30	0	p26f0-n30-01f1	r26f0-n30-01f1	t26f0-n30-01f1
27	manikin				ref.mic	mic-1	1	0	0	45	p27f0-0-45f1f1	r27f0-0-45f1f1	t27f0-0-45f1f1
28	manikin				ref.mic	mic-1	1	45	-45	0	p28f45-n45-01f1f1	r28f45-n45-01f1f1	t28f45-n45-01f1f1
29	manikin				ref.mic	mic-1	1	-30	0	0	p29fn30-0-01f1	r29fn30-0-01f1	t29fn30-0-01f1
30		manikin			ref.mic	mic-1	1	0	0	0	p30f0-0-02f1	r30f0-0-02f1	t30f0-0-02f1
31		manikin			ref.mic	mic-1	1	-32.3	0	0	p31fn32-0-02f1	r31fn32-0-02f1	t31fn32-0-02f1
32		manikin			ref.mic	mic-1	2	0	0	0	p32f0-0-02f2	r32f0-0-02f2	t32f0-0-02f2
33		manikin			ref.mic	mic-1	2	-32.3	0	0	p33fn32-0-02f2	r33fn32-0-02f2	t33fn32-0-02f2
34		manikin			ref.mic	mic-1	2	-32.3	30	0	p34fn32-30-02f2	r34fn32-30-02f2	t34fn32-30-02f2
35			manikin		ref.mic	mic-1	2	-45	0	0	p35fn45-0-03f2	r35fn45-0-03f2	t35fn45-0-03f2 1
36	bformat	mic-1			ref.mic		2				p36bmlf2f2	r36bmlf2f2	t36bmlf2f2 2
37	bformat	mic-1			ref.mic		1				p37bmlf2f1	r37bmlf2f1	t37bmlf2f1 2
38	mic-1	bformat			ref.mic		1				p38bmlf2f1f1	r38bmlf2f1f1	t38bmlf2f1f1 2
39	mic-1	bformat			ref.mic		2				p39bmlf2f1f2input10v	r39bmlf2f1f2	t39bmlf2f1f2 2,3
40			bformat	mic-1	ref.mic		2				p40bmlf34f2input10vgain20dBZ	r40bmlf34f2input10vgain20dBZ	t40bmlf34f2gain20dBZ 2,3,4,5
41			mic-1	bformat	ref.mic		2				p41bmlf43f2input10v	r41bmlf43f2input10v	t41bmlf43f2 2,3,4
42			mic-1	bformat	ref.mic		1				p42bmlf43f1input10v	r42bmlf43f1input10v	t42bmlf43f1 2,3,4
43			bformat	mic-1	ref.mic		1				p43bmlf34f1input10vgain20dBZ	r43bmlf34f1input10vgain20dBZ	t43bmlf34f1gain20dBZ 2,3,4,5

Table 12. Special measurement conditions for the binaural tests

- 1)An additional gain of 20 dB was applied to the mannequin microphone output signals for test 35 only
- 2)The microphone mic-1 was changed from a pressure microphone to a free-field microphone for tests 36-43
- 3)The pulse input signal was changed from 4 V to 10 V for tests 39-43
- 4)The pseudo random time input signals were changed from 4 V to 10 V for tests 40-43 and 1a-47a
- 5)An additional gain of 20 dB was applied to the Y and Z channels of the B-format microphone for tests 40 and 43

Table 13. Channel calibration settings

Channel	Transducer	Unit	Gain [dB]	Sensitivity [mV/EU]	Tests
1.	force	N	0	22.471	1-43; 1a-47a
2.	accel 1	m/s ²	0	10.3807	1-43; 1a-47a
3.	accel 2	m/s ²	0	1.05031	1-43; 1a-47a
4.	accel 3	m/s ²	0	1.05031	1-43; 1a-47a
5.	accel 4	m/s ²	0	1.08090	1-43; 1a-47a
6.	accel 5	m/s ²	40	1.05031	1-43; 1a-47a
7.	ref.mic (pressure)	Pa	20	8.54757	1-35
7.	ref.mic (pressure)	Pa	20	9.29095	36-43; 1a-47a
8.	mic-1 (pressure)	Pa	20	9.34275	1-35
8.	mic-1 (free field)	Pa	20	38.3264	36-43; 1a-47a
9.	manikin left	Pa	10	132.32	1-43; 1a-47a
10.	manikin right	Pa	10	133.318	1-43; 1a-47a
11.	B-format W	Pa	0	158.114	1-43; 1a-47a
12.	B-format X	Pa	0	223.342	1-43; 1a-47a
13.	B-format Y	Pa	0	223.342	1-43; 1a-47a
14.	B-format Z	Pa	0	223.342	1-43; 1a-47a

Table 14. Initial data acquisition sampling, trigger, window, averaging, filter and measurement conditions

	Pulse excitation	Random excitation	Pseudo-random excitation
Spectral lines	6401	6401	6401
Delta frequency	0.625 Hz	0.625 Hz	0.625 Hz
Maximum frequency	4000.0 Hz	4000.0 Hz	4000.0 Hz
Minimum frequency	0 Hz	0 Hz	0 Hz
Frame size	16384	16384	16384
Frame length	1.6 sec	1.6 sec	1.6 sec
Delta time	9.77E-05 sec	9.77E-05 sec	9.77E-05 sec
Sampling frequency	10240.0 Hz	10240.0 Hz	10240.0 Hz
Trigger method	First frame	First frame	Every frame
Trigger source	Manual	Manual	Shaker
Trigger level	Off	Off	10%
Window	None	None	Hanning narrow
Averaging method	Stable	Stable	Stable
Exponential average constant	5	5	5
Frames per average	3	5	10
Low-pass filter	No	2000 Hz	No
Time history	Yes	Yes	No
Auto spectrum	No	No	Yes
Transfer function	No	No	Yes
Coherence	No	No	Yes

Table 15. Binaural test matrix for measurements with the reflective surface
in the anechoic room of the SALT facility

BINAURAL TEST MATRIX IN THE ANECHOIC ROOM OF THE SALT FACILITY										REFLECTIVE SURFACE			
	<--- anechoic chamber locations --->						shaker	<--- mannequin --->				file names	
test	loc.1	loc.2	loc.3	loc.4	loc.7	b.psi	ploc.	phi.1	phi.2	phi.3	pulse (.ati)	random (.ati)	transfer (.afu)
1a	manikin				ref.mic		2	0	0	0	ap1f0-0-0i1f2	ar1f0-0-0i1f2	at1f0-0-0i1f2
2a	manikin				ref.mic		2	30	0	0	ap2f0-30-0i1f2	ar2f0-30-0i1f2	at2f0-30-0i1f2
3a	manikin				ref.mic		2	90	0	0	ap3f0-90-0i1f2	ar3f0-90-0i1f2	at3f0-90-0i1f2
4a	manikin				ref.mic		2	150	0	0	ap4f0-150-0i1f2	ar4f0-150-0i1f2	at4f0-150-0i1f2
5a	manikin				ref.mic		2	0	30	0	ap5f0-30-0i1f2	ar5f0-30-0i1f2	at5f0-30-0i1f2
6a	manikin				ref.mic		2	0	-30	0	ap6f0-n30-0i1f2	ar6f0-n30-0i1f2	at6f0-n30-0i1f2
7a	manikin				ref.mic		2	0	0	45	ap7f0-0-45i1f2	ar7f0-0-45i1f2	at7f0-0-45i1f2
8a	manikin				ref.mic		2	45	-45	0	ap8f45-n45-0i1f2	ar8f45-n45-0i1f2	at8f45-n45-0i1f2
9a	manikin				ref.mic		2	-30	0	0	ap9fn30-0-0i1f2	ar9fn30-0-0i1f2	at9fn30-0-0i1f2
10a	manikin				ref.mic		2	-115	20	0	ap10fn115-20-0i1f2	ar10fn115-20-0i1f2	at10fn115-20-0i1f2
11a	manikin				ref.mic		2	-45	0	0	ap11fn45-0-0i1f2	ar11fn45-0-0i1f2	at11fn45-0-0i1f2
12a	manikin				ref.mic		2	45	-40	0	ap12f45-n40-0i1f2	ar12f45-n40-0i1f2	at12f45-n40-0i1f2
13a	manikin				ref.mic		2	0	-80	0	ap13f0-n80-0i1f2	ar13f0-n80-0i1f2	at13f0-n80-0i1f2
14a	manikin				ref.mic		2	180	0	0	ap14f180-0-0i1f2	ar14f180-0-0i1f2	at14f180-0-0i1f2
15a	manikin				ref.mic		2	-90	0	0	ap15fn90-0-0i1f2	ar15fn90-0-0i1f2	at15fn90-0-0i1f2
16a	manikin				ref.mic		2	-150	0	0	ap16fn150-0-0i1f2	ar16fn150-0-0i1f2	at16fn150-0-0i1f2
17a	manikin				ref.mic		2	45	0	0	ap17f45-0-0i1f2	ar17f45-0-0i1f2	at17f45-0-0i1f2
18a	manikin				ref.mic		2	-115	-20	0	ap18fn115-n20-0i1f2	ar18fn115-n20-0i1f2	at18fn115-n20-0i1f2
19a	manikin				ref.mic		2	45	20	0	ap19f45-20-0i1f2	ar19f45-20-0i1f2	at19f45-20-0i1f2
20a	manikin				ref.mic		2	45	-20	0	ap20f45-n20-0i1f2	ar20f45-n20-0i1f2	at20f45-n20-0i1f2
21a	manikin				ref.mic		1	0	0	0	ap21f0-0-0i1f1	ar21f0-0-0i1f1	at21f0-0-0i1f1
22a	manikin				ref.mic		1	0	30	0	ap22f0-30-0i1f1	ar22f0-30-0i1f1	at22f0-30-0i1f1
23a	manikin				ref.mic		1	30	0	0	ap23f30-0-0i1f1	ar23f30-0-0i1f1	at23f30-0-0i1f1
24a	manikin				ref.mic		1	90	0	0	ap24f90-0-0i1f1	ar24f90-0-0i1f1	at24f90-0-0i1f1
25a	manikin				ref.mic		1	150	0	0	ap25f150-0-0i1f1	ar25f150-0-0i1f1	at25f150-0-0i1f1
26a	manikin				ref.mic		1	0	-30	0	ap26f0-n30-0i1f1	ar26f0-n30-0i1f1	at26f0-n30-0i1f1
27a	manikin				ref.mic		1	0	0	45	ap27f0-0-45i1f1	ar27f0-0-45i1f1	at27f0-0-45i1f1
28a	manikin				ref.mic		1	45	-45	0	ap28f45-n45-0i1f1	ar28f45-n45-0i1f1	at28f45-n45-0i1f1
29a	manikin				ref.mic		1	-30	0	0	ap29fn30-0-0i1f1	ar29fn30-0-0i1f1	at29fn30-0-0i1f1
30a		manikin			ref.mic		1	0	0	0	ap30f0-0-0i2f1	ar30f0-0-0i2f1	at30f0-0-0i2f1
31a		manikin			ref.mic		1	-32.3	0	0	ap31fn32-0-0i2f1	ar31fn32-0-0i2f1	at31fn32-0-0i2f1
32a		manikin			ref.mic		2	0	0	0	ap32f0-0-0i2f2	ar32f0-0-0i2f2	at32f0-0-0i2f2
33a		manikin			ref.mic		2	-32.3	0	0	ap33fn32-0-0i2f2	ar33fn32-0-0i2f2	at33fn32-0-0i2f2
34a		manikin			ref.mic		2	-32.3	30	0	ap34fn32-30-0i2f2	ar34fn32-30-0i2f2	at34fn32-30-0i2f2
36a	bformat	mic-1			ref.mic		2				ap36bml12f2	ar36bml12f2	at36bml12f2
37a	bformat	mic-1			ref.mic		1				ap37bml12f1	ar37bml12f1	at37bml12f1
38a	mic-1	bformat			ref.mic		1				ap38bml21f1	ar38bml21f1	at38bml21f1
39a	mic-1	bformat			ref.mic		2				ap39bml21f2input10v	ar39bml21f2	at39bml21f2
44a	bformat					0	2				ap44b000f-0-0-0i12f1	ar44b000f-0-0-0i12f1	at44b000f-0-0-0i12f1
45a	bformat					90	2				ap45b090f-0-0-0i12f1	ar45b090f-0-0-0i12f1	at45b090f-0-0-0i12f1
46a	bformat					180	2				ap46b180f-0-0-0i12f1	ar46b180f-0-0-0i12f1	at46b180f-0-0-0i12f1
47a	bformat					270	2				ap47b270f-0-0-0i12f1	ar47b270f-0-0-0i12f1	at47b270f-0-0-0i12f1

Table 16. Files archived on compact disk 8

Compact Disk 8: 388 MB	(Compressed ZIP file: 204MB)	
t10fn115-20-011f2.afu	p10fn115-20-011f2.ati	r10fn115-20-011f2.ati
t11fn45-0-011f2.afu	p11fn45-0-011f2.ati	r11fn45-0-011f2.ati
t12f45-n40-011f2.afu	p12f45-n40-011f2.ati	r12f45-n40-011f2.ati
t13f0-n80-011f2.afu	p13f0-n80-011f2.ati	r13f0-n80-011f2.ati
t14f180-0-011f2.afu	p14f180-0-011f2.ati	r14f180-0-011f2.ati
t15fn90-0-011f2.afu	p15fn90-0-011f2.ati	r15fn90-0-011f2.ati
t16fn150-0-011f2.afu	p16fn150-0-011f2.ati	r16fn150-0-011f2.ati
t17f45-0-011f2.afu	p17f45-0-011f2.ati	r17f45-0-011f2.ati
t18fn115-n20-011f2.afu	p18fn115-n20-011f2.ati	r18fn115-n20-011f2.ati
t19f45-20-011f2.afu	p19f45-20-011f2.ati	r19f45-20-011f2.ati
t1f0-0-011f2.afu	p1f0-0-011f2.ati	r1f0-0-011f2.ati
t20f45-n20-011f2.afu	p20f45-n20-011f2.ati	r20f45-n20-011f2.ati
t21f0-0-011f1.afu	p21f0-0-011f1.ati	r21f0-0-011f1.ati
t22f0-30-011f1.afu	p22f0-30-011f1.ati	r22f0-30-011f1.ati
t23f30-0-011f1.afu	p23f30-0-011f1.ati	r23f30-0-011f1.ati
t24f90-0-011f1.afu	p24f90-0-011f1.ati	r24f90-0-011f1.ati
t25f150-0-011f1.afu	p25f150-0-011f1.ati	r25f150-0-011f1.ati
t26f0-n30-011f1.afu	p26f0-n30-011f1.ati	r26f0-n30-011f1.ati
t27f0-0-4511f1.afu	p27f0-0-4511f1.ati	r27f0-0-4511f1.ati
t28f45-n45-011f1.afu	p28f45-n45-011f1.ati	r28f45-n45-011f1.ati
t29fn30-0-011f1.afu	p29fn30-0-011f1.ati	r29fn30-0-011f1.ati
t2f0-30-011f2.afu	p2f0-30-011f2.ati	r2f0-30-011f2.ati
t30f0-0-012f1.afu	p30f0-0-012f1.ati	r30f0-0-012f1.ati
t31fn32-0-012f1.afu	p31fn32-0-012f1.ati	r31fn32-0-012f1.ati
t32f0-0-012f2.afu	p32f0-0-012f2.ati	r32f0-0-012f2.ati
t33fn32-0-012f2.afu	p33fn32-0-012f2.ati	r33fn32-0-012f2.ati
t34fn32-30-012f2.afu	p34fn32-30-012f2.ati	r34fn32-30-012f2.ati
t35fn45-0-013f2.afu	p35fn45-0-013f2.ati	r35fn45-0-013f2.ati
t36bml12f2.afu	p36bml12f2.ati	r36bml12f2.ati
t37bml12f1.afu	p37bml12f1.ati	r37bml12f1.ati
t38bml21f1.afu	p38bml21f1.ati	r38bml21f1.ati
t39bml21f2.afu	p39bml21f2input10v.ati	r39bml21f2.ati
t3f0-90-011f2.afu	p3f0-90-011f2.ati	r3f0-90-011f2.ati
t40bml34f2.afu	p40bml34f2input10vgain20dBYZ.ati	r40bml34f2input10v.ati
t40bml34f2gain20dBYZ.afu	p41bml43f2input10v.ati	r40bml34f2input10vgain20dBYZ.ati
t41bml43f2.afu	p42bml43f1input10v.ati	r41bml43f2input10v.ati
t42bml43f1.afu	p43bml34f1input10vgain20dBYZ.ati	r42bml43f1input10v.ati
t43bml34f1.afu	p4f0-150-011f2.ati	r43bml34f1input10v.ati
t43bml34f1gain20dBYZ.afu	p5f0-30-011f2.ati	r43bml34f1input10vgain20dBYZ.ati
t4f0-150-011f2.afu	p6f0-n30-011f2.ati	r4f0-150-011f2.ati
t5f0-30-011f2.afu	p7f0-0-4511f2.ati	r5f0-30-011f2.ati
t6f0-n30-011f2.afu	p8f45-n45-011f2.ati	r6f0-n30-011f2.ati
t7f0-0-4511f2.afu	p9fn30-0-011f2.ati	r7f0-0-4511f2.ati
t8f45-n45-011f2.afu	sinfun.ati	r8f45-n45-011f2.ati
t9fn30-0-011f2.afu	t25f150-0-011f1background.afu	r9fn30-0-011f2.ati

Table 17. Files archived on compact disk 9

Compact Disk 9: 359 MB (Compressed ZIP file: 185 MB)		
at10fn115-20-011f2.afu	ap10fn115-20-011f2.ati	ar10fn115-20-011f2.ati
at11fn45-0-011f2.afu	ap11fn45-0-011f2.ati	ar11fn45-0-011f2.ati
at12f45-n40-011f2.afu	ap12f45-n40-011f2.ati	ar12f45-n40-011f2.ati
at13f0-n80-011f2.afu	ap13f0-n80-011f2.ati	ar13f0-n80-011f2.ati
at14f180-0-011f2.afu	ap14f180-0-011f2.ati	ar14f180-0-011f2.ati
at15fn90-0-011f2.afu	ap15fn90-0-011f2.ati	ar15fn90-0-011f2.ati
at16fn150-0-011f2.afu	ap16fn150-0-011f2.ati	ar16fn150-0-011f2.ati
at17f45-0-011f2.afu	ap17f45-0-011f2.ati	ar17f45-0-011f2.ati
at18fn115-n20-011f2.afu	ap18fn115-n20-011f2.ati	ar18fn115-n20-011f2.ati
at19f45-20-011f2.afu	ap19f45-20-011f2.ati	ar19f45-20-011f2.ati
at1f0-0-011f2.afu	ap1f0-0-011f2.ati	ar1f0-0-011f2.ati
at20f45-n20-011f2.afu	ap20f45-n20-011f2.ati	ar20f45-n20-011f2.ati
at21f0-0-011f1.afu	ap21f0-0-011f1.ati	ar21f0-0-011f1.ati
at22f0-30-011f1.afu	ap22f0-30-011f1.ati	ar22f0-30-011f1.ati
at23f30-0-011f1.afu	ap23f30-0-011f1.ati	ar23f30-0-011f1.ati
at24f90-0-011f1.afu	ap24f90-0-011f1.ati	ar24f90-0-011f1.ati
at25f150-0-011f1.afu	ap25f150-0-011f1.ati	ar25f150-0-011f1.ati
at26f0-n30-011f1.afu	ap26f0-n30-011f1.ati	ar26f0-n30-011f1.ati
at27f0-0-451f1.afu	ap27f0-0-451f1.ati	ar27f0-0-451f1.ati
at28f45-n45-011f1.afu	ap28f45-n45-011f1.ati	ar28f45-n45-011f1.ati
at29fn30-0-011f1.afu	ap29fn30-0-011f1.ati	ar29fn30-0-011f1.ati
at2f0-30-011f2.afu	ap2f0-30-011f2.ati	ar2f0-30-011f2.ati
at30f0-0-012f1.afu	ap30f0-0-012f1.ati	ar30f0-0-012f1.ati
at31fn32-0-012f1.afu	ap31fn32-0-012f1.ati	ar31fn32-0-012f1.ati
at32f0-0-012f2.afu	ap32f0-0-012f2.ati	ar32f0-0-012f2.ati
at33fn32-0-012f2.afu	ap33fn32-0-012f2.ati	ar33fn32-0-012f2.ati
at34fn32-30-012f2.afu	ap34fn32-30-012f2.ati	ar34fn32-30-012f2.ati
at36bml12f2.afu	ap36bml12f2.ati	ar36bml12f2.ati
at37bml12f1.afu	ap37bml12f1.ati	ar37bml12f1.ati
at38bml21f1.afu	ap38bml21f1.ati	ar38bml21f1.ati
at39bml21f2.afu	ap39bml21f2.ati	ar39bml21f2.ati
at3f0-90-011f2.afu	ap3f0-90-011f2.ati	ar3f0-90-011f2.ati
at44b000f-0-0-0112f1.afu	ap44b000f-0-0-0112f1.ati	ar44b000f-0-0-0112f1.ati
at45b090f-0-0-0112f1.afu	ap45b090f-0-0-0112f1.ati	ar45b090f-0-0-0112f1.ati
at46b180f-0-0-0112f1.afu	ap46b180f-0-0-0112f1.ati	ar46b180f-0-0-0112f1.ati
at47b270f-0-0-0112f1.afu	ap47b270f-0-0-0112f1.ati	ar47b270f-0-0-0112f1.ati
at4f0-150-011f2.afu	ap4f0-150-011f2.ati	ar4f0-150-011f2.ati
at5f0-30-011f2.afu	ap5f0-30-011f2.ati	ar5f0-30-011f2.ati
at6f0-n30-011f2.afu	ap6f0-n30-011f2.ati	ar6f0-n30-011f2.ati
at7f0-0-451f2.afu	ap7f0-0-451f2.ati	ar7f0-0-451f2.ati
at8f45-n45-011f2.afu	ap8f45-n45-011f2.ati	ar8f45-n45-011f2.ati
at9fn30-0-011f2.afu	ap9fn30-0-011f2.ati	ar9fn30-0-011f2.ati

Table 18. Files archived on compact disk 10

Compact Disk 10: 642 MB (Compressed ZIP file: 164 MB)		
r10fn115-20-011f2.unv	r23f30-0-011f1.unv	r37bml12f1.unv
r11fn45-0-011f2.unv	r24f90-0-011f1.unv	r38bml21f1.unv
r12f45-n40-011f2.unv	r25f150-0-011f1.unv	r39bml21f2.unv
r13f0-n80-011f2.unv	r26f0-n30-011f1.unv	r3f0-90-011f2.unv
r14f180-0-011f2.unv	r27f0-0-4511f1.unv	r40bml34f2input10v.unv
r15fn90-0-011f2.unv	r28f45-n45-011f1.unv	r40bml34f2input10vgain20dBYZ.unv
r16fn150-0-011f2.unv	r29fn30-0-011f1.unv	r42bml43f1input10v.unv
r17f45-0-011f2.unv	r2f0-30-011f2.unv	r43bml34f1input10v.unv
r18fn115-n20-011f2.unv	r30f0-0-012f1.unv	r43bml34f1input10vgain20dBYZ.unv
r19f45-20-011f2.unv	r31fn32-0-012f1.unv	r4f0-150-011f2.unv
r1f0-0-011f2.unv	r32f0-0-012f2.unv	r5f0-30-011f2repeat.unv
r20f45-n20-011f2.unv	r33fn32-0-012f2.unv	r6f0-n30-011f2.unv
r21f0-0-011f1.unv	r34fn32-30-012f2.unv	r7f0-0-4511f2.unv
r22f0-30-011f1.unv	r35fn45-0-013f2.unv	r8f45-n45-011f2.unv
	r36bml12f2.unv	r9fn30-0-011f2.unv

Table 19. Files archived on compact disk 11

Compact Disk 11: 598 MB (Compressed ZIP file: 125 MB)		
p10fn115-20-011f2.unv	p38bml21f1.unv	t25f150-0-011f1.unv
p11fn45-0-011f2.unv	p3f0-90-011f2.unv	t25f150-0-011f1background.unv
p12f45-n40-011f2.unv	p40bml34f2input10vgain20dBYZ.unv	t26f0-n30-011f1.unv
p13f0-n80-011f2.unv	p41bml43f2input10v.unv	t30f0-0-012f1.unv
p14f180-0-011f2.unv	p42bml43f1input10v.unv	t27f0-0-4511f1.unv
p15fn90-0-011f2.unv	p43bml34f1input10vgain20dBYZ.unv	t28f45-n45-011f1.unv
p16fn150-0-011f2.unv	p4f0-150-011f2.unv	t29fn30-0-011f1.unv
p17f45-0-011f2.unv	p5f0-30-011f2repeat.unv	t2f0-30-011f2.unv
p18fn115-n20-011f2.unv	p6f0-n30-011f2repeat.unv	t31fn32-0-012f1.unv
p19f45-20-011f2.unv	p7f0-0-4511f2.unv	t32f0-0-012f2.unv
p1f0-0-011f2.unv	p8f45-n45-011f2.unv	t33fn32-0-012f2.unv
p20f45-n20-011f2.unv	p9fn30-0-011f2.unv	t34fn32-30-012f2.unv
p21f0-0-011f1.unv	r5f0-30-011f2repeat.unv	t35fn45-0-013f2.unv
p22f0-30-011f1.unv	sincfun.unv	t36bml12f2.unv
p23f30-0-011f1.unv	t10fn115-20-011f2.unv	t37bml12f1.unv
p24f90-0-011f1.unv	t11fn45-0-011f2.unv	t38bml21f1.unv
p25f150-0-011f1.unv	t12f45-n40-011f2.unv	t39bml21f2.unv
p26f0-n30-011f1.unv	t13f0-n80-011f2.unv	t3f0-90-011f2.unv
p27f0-0-4511f1.unv	t14f180-0-011f2.unv	t40bml34f2.unv
p28f45-n45-011f1.unv	t15fn90-0-011f2.unv	t40bml34f2gain20dBYZ.unv
p29fn30-0-011f1.unv	t16fn150-0-011f2.unv	t41bml43f2.unv
p2f0-30-011f2.unv	t17f45-0-011f2.unv	t42bml43f1.unv
p30f0-0-012f1.unv	t18fn115-n20-011f2.unv	t43bml34f1.unv
p31fn32-0-012f1.unv	t19f45-20-011f2.unv	t43bml34f1gain20dBYZ.unv
p32f0-0-012f2.unv	t1f0-0-011f2.unv	t4f0-150-011f2.unv
p33fn32-0-012f2.unv	t20f45-n20-011f2.unv	t5f0-30-011f2.unv
p34fn32-30-012f2.unv	t21f0-0-011f1.unv	t6f0-n30-011f2.unv
p35fn45-0-013f2.unv	t22f0-30-011f1.unv	t7f0-0-4511f2.unv
p36bml12f2.unv	t23f30-0-011f1.unv	t8f45-n45-011f2.unv
p37bml12f1.unv	t24f90-0-011f1.unv	t9fn30-0-011f2.unv

Table 20. Files archived on compact disk 12

Compact Disk 12: 613 MB (Compressed ZIP file: 154 MB)		
ar10fn115-20-011f2.unv	ar23f30-0-011f1.unv	ar37bml12f1.unv
ar11fn45-0-011f2.unv	ar24f90-0-011f1.unv	ar38bml21f1.unv
ar12f45-n40-011f2.unv	ar25f150-0-011f1.unv	ar39bml21f2.unv
ar13f0-n80-011f2.unv	ar26f0-n30-011f1.unv	ar3f0-90-011f2.unv
ar14f180-0-011f2.unv	ar27f0-0-4511f1.unv	ar44b000f-0-0-0112f1.unv
ar15fn90-0-011f2.unv	ar28f45-n45-011f1.unv	ar45b090f-0-0-0112f1.unv
ar16fn150-0-011f2.unv	ar29fn30-0-011f1.unv	ar46b180f-0-0-0112f1.unv
ar17f45-0-011f2.unv	ar2f0-30-011f2.unv	ar47b270f-0-0-0112f1.unv
ar18fn115-n20-011f2.unv	ar30f0-0-012f1.unv	ar4f0-150-011f2.unv
ar19f45-20-011f2.unv	ar31fn32-0-012f1.unv	ar5f0-30-011f2.unv
ar1f0-0-011f2.unv	ar32f0-0-012f2.unv	ar6f0-n30-011f2.unv
ar20f45-n20-011f2.unv	ar33fn32-0-012f2.unv	ar7f0-0-4511f2.unv
ar21f0-0-011f1.unv	ar34fn32-30-012f2.unv	ar8f45-n45-011f2.unv
ar22f0-30-011f1.unv	ar36bml12f2.unv	ar9fn30-0-011f2.unv

Table 21. Files archived on compact disk 13

Compact Disk 12: 597 MB (Compressed ZIP file: 118 MB)		
ap10fn115-20-011f2.unv	ap39bml21f2.unv	at26f0-n30-011f1.unv
ap11fn45-0-011f2.unv	ap3f0-90-011f2.unv	at27f0-0-4511f1.unv
ap12f45-n40-011f2.unv	ap44b000f-0-0-0112f1.unv	at28f45-n45-011f1.unv
ap13f0-n80-011f2.unv	ap45b090f-0-0-0112f1.unv	at29fn30-0-011f1.unv
ap14f180-0-011f2.unv	ap46b180f-0-0-0112f1.unv	at2f0-30-011f2.unv
ap15fn90-0-011f2.unv	ap47b270f-0-0-0112f1.unv	at30f0-0-012f1.unv
ap16fn150-0-011f2.unv	ap4f0-150-011f2.unv	at31fn32-0-012f1.unv
ap17f45-0-011f2.unv	ap5f0-30-011f2.unv	at32f0-0-012f2.unv
ap18fn115-n20-011f2.unv	ap6f0-n30-011f2.unv	at33fn32-0-012f2.unv
ap19f45-20-011f2.unv	ap7f0-0-4511f2.unv	at34fn32-30-012f2.unv
ap1f0-0-011f2.unv	ap8f45-n45-011f2.unv	at36bml12f2.unv
ap20f45-n20-011f2.unv	ap9fn30-0-011f2.unv	at37bml12f1.unv
ap21f0-0-011f1.unv	at10fn115-20-011f2.unv	at38bml21f1.unv
ap22f0-30-011f1.unv	at11fn45-0-011f2.unv	at39bml21f2.unv
ap23f30-0-011f1.unv	at12f45-n40-011f2.unv	at3f0-90-011f2.unv
ap24f90-0-011f1.unv	at13f0-n80-011f2.unv	at44b000f-0-0-0112f1.unv
ap25f150-0-011f1.unv	at14f180-0-011f2.unv	at45b090f-0-0-0112f1.unv
ap26f0-n30-011f1.unv	at15fn90-0-011f2.unv	at46b180f-0-0-0112f1.unv
ap27f0-0-4511f1.unv	at16fn150-0-011f2.unv	at47b270f-0-0-0112f1.unv
ap28f45-n45-011f1.unv	at17f45-0-011f2.unv	at4f0-150-011f2.unv
ap29fn30-0-011f1.unv	at18fn115-n20-011f2.unv	at5f0-30-011f2.unv
ap2f0-30-011f2.unv	at19f45-20-011f2.unv	at6f0-n30-011f2.unv
ap30f0-0-012f1.unv	at1f0-0-011f2.unv	at7f0-0-4511f2.unv
ap31fn32-0-012f1.unv	at20f45-n20-011f2.unv	at8f45-n45-011f2.unv
ap32f0-0-012f2.unv	at21f0-0-011f1.unv	at9fn30-0-011f2.unv
ap33fn32-0-012f2.unv	at22f0-30-011f1.unv	p5f0-30-011f2repeat.unv
ap34fn32-30-012f2.unv	at23f30-0-011f1.unv	p6f0-n30-011f2repeat.unv
ap36bml12f2.unv	at24f90-0-011f1.unv	r5f0-30-011f2repeat.unv
ap37bml12f1.unv	at25f150-0-011f1.unv	sincfun.unv
ap38bml21f1.unv		

Figures

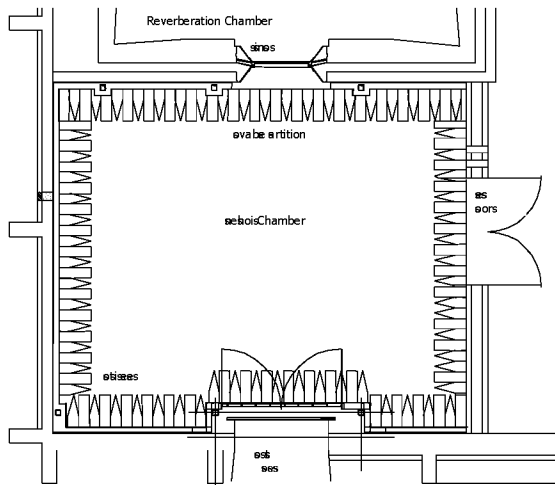


Figure 1. Reverberation chamber, anechoic chamber and the transmission loss window of the Structural Acoustics Transmission and Loads (SALT) facility.

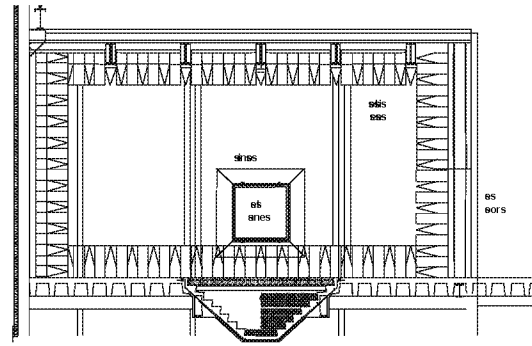


Figure 2. Cross-sectional view of the anechoic chamber showing the transmission loss window. (The stairwell was filled with absorptive materials and covered by a slab of concrete.)



Figure 3. Reverberant chamber view of the aluminum panel installed in the transmission loss window.

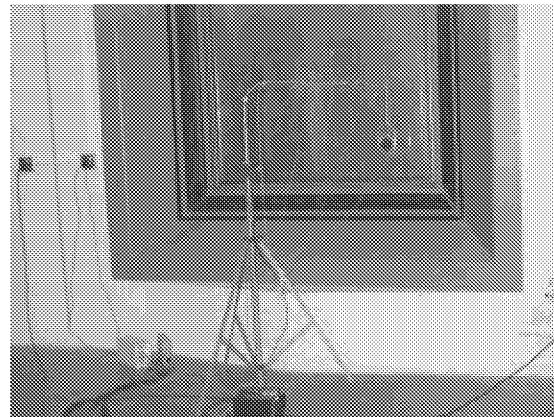


Figure 4. View of the 4.9-mm thick aluminum panel with the force and accelerometer transducers of the mini shaker at location ploc.2, three accelerometers on the panel and one accelerometer mounted on the frame.

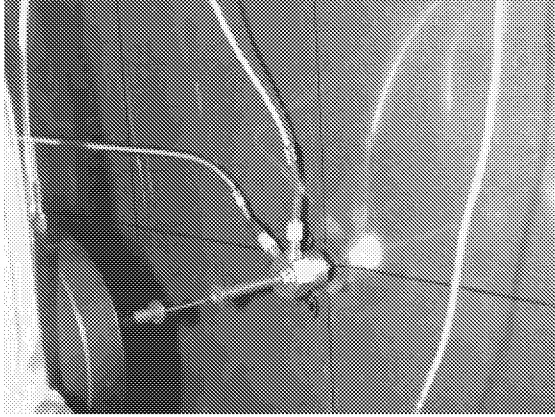


Figure 5. Close-up view of the combined force and accelerometer transducers of the mini shaker.

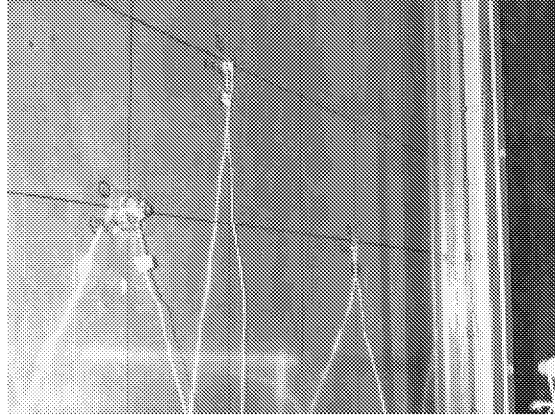


Figure 6. Close-up view of the three accelerometers mounted on the aluminum panel.

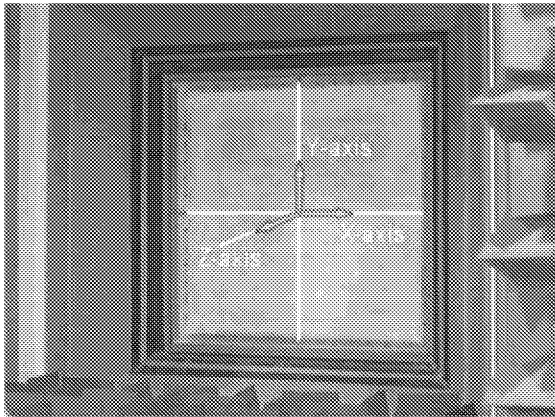


Figure 7. Cartesian panel coordinate system.

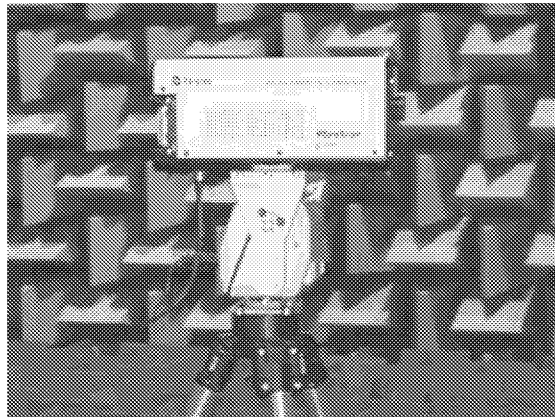


Figure 8. Close-up of the scanning laser vibrometer.

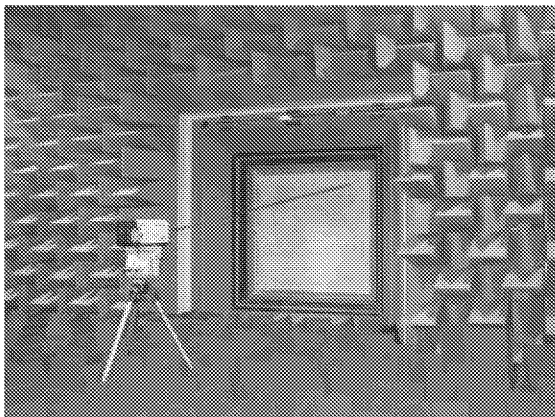


Figure 9. The scanning laser vibrometer measuring the two-dimensional distribution of vibrational panel velocities.

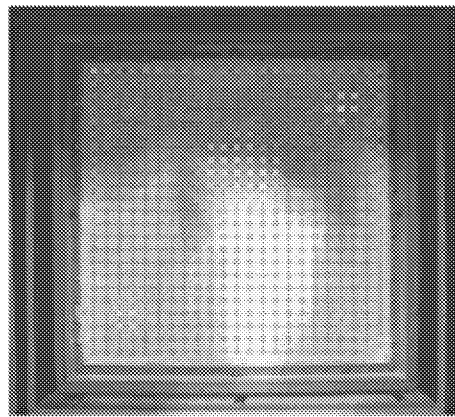


Figure 10. The 23 by 23 measurement grid superimposed on the video image taken by the laser vibrometer system.

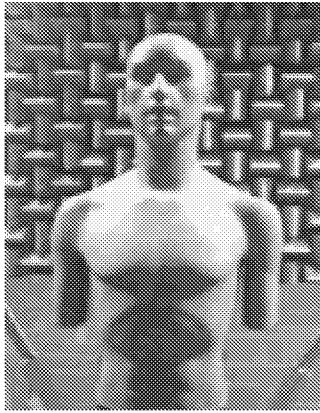


Figure 11. The Knowles Electronics Manikin for Acoustic Research (KEMAR).

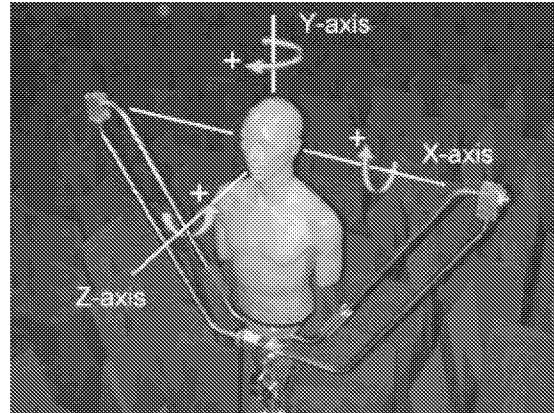


Figure 12. Local mannequin Cartesian coordinate system and the positive rotation directions.

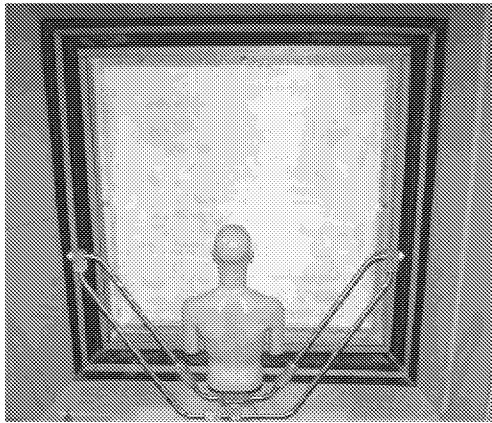


Figure 13. The Z-axis of the mannequin aligned with the center of the test panel (Test 1 in Table 11).

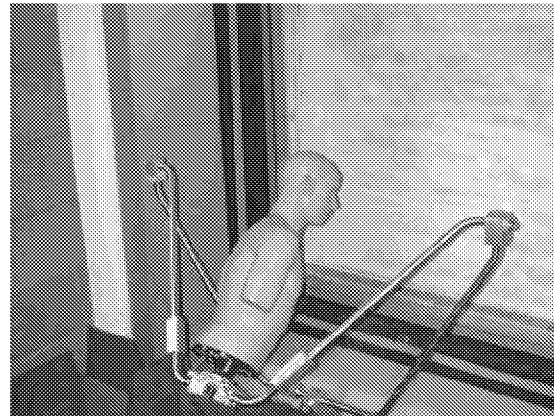


Figure 14. The KEMAR mannequin rotated 45 degrees about the Y-axis and minus 45 degrees about the X-axis (Test 8 in Table 11).

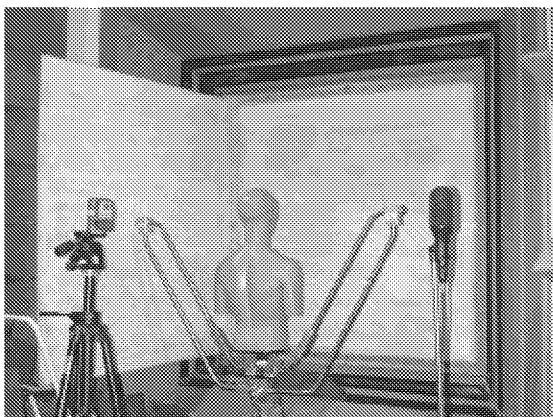


Figure 15. A reflective panel added to the test set-up (Test 1a in Table 15) with a laser alignment tool on the left and the B-format microphone on the right.

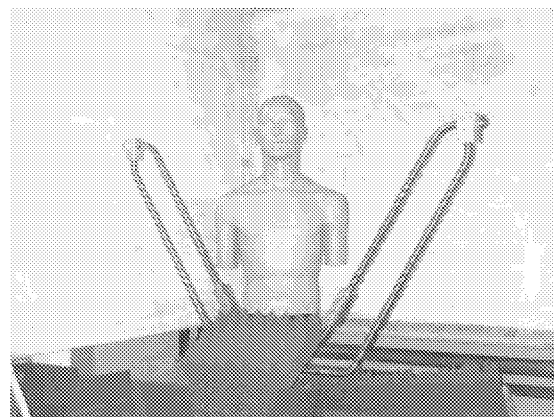


Figure 16. The mannequin rotated 150 degrees about the Y-axis (Test 4a in Table 15).

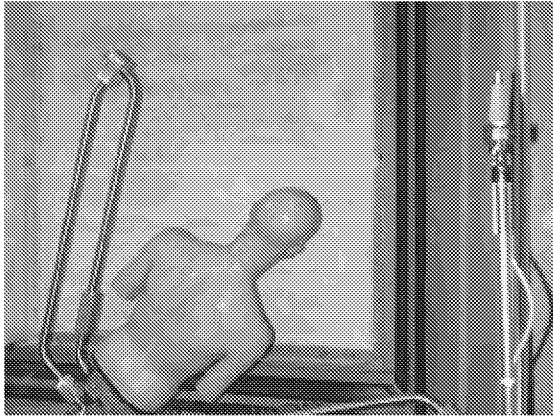


Figure 17. The mannequin rotated 45 degrees about the Z-axis (Test 7a in Table 15).

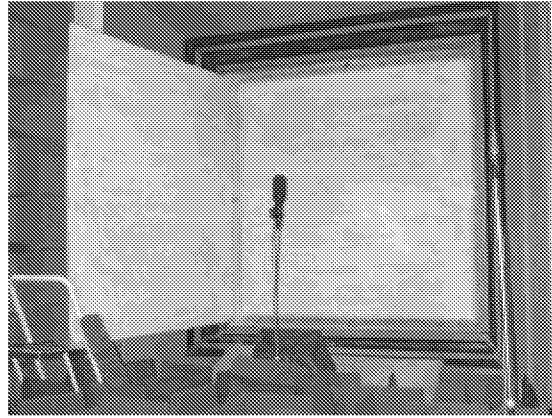


Figure 18. B-format microphone at measurement location loc.1 (Test 36a in Table 15).

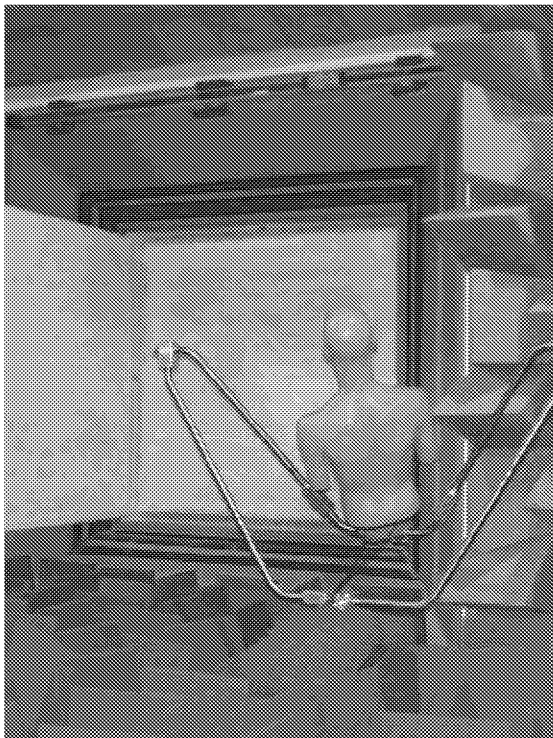


Figure 19. The mannequin at location loc.2 rotated minus 32.3 degrees about the Y-axis and 30 degrees about the X-axis (Test 34a in Table 15).



Figure 20. View of the B-format microphone at measurement location loc.1 with the mannequin in the foreground at measurement location loc.2.

REPORT DOCUMENTATION PAGE			Form Approved OMB No. 0704-0188	
Public reporting burden for this collection of information is estimated to average 1 hour per response, including the time for reviewing instructions, searching existing data sources, gathering and maintaining the data needed, and completing and reviewing the collection of information. Send comments regarding this burden estimate or any other aspect of this collection of information, including suggestions for reducing this burden, to Washington Headquarters Services, Directorate for Information Operations and Reports, 1215 Jefferson Davis Highway, Suite 1204, Arlington, VA 22202-4302, and to the Office of Management and Budget, Paperwork Reduction Project (0704-0188), Washington, DC 20503.				
1. AGENCY USE ONLY (Leave blank)		2. REPORT DATE December 2001		3. REPORT TYPE AND DATES COVERED Contractor Report
4. TITLE AND SUBTITLE Binaural Simulation Experiments in the NASA Langley Structural Acoustics Loads and Transmission Facility			5. FUNDING NUMBERS NAS1-00135 WU 705-30-11-13	
6. AUTHOR(S) Ferdinand W. Grosveld				
7. PERFORMING ORGANIZATION NAME(S) AND ADDRESS(ES) Lockheed Martin Engineering and Sciences NASA Langley Research Center Hampton, Virginia 23681-2199			8. PERFORMING ORGANIZATION REPORT NUMBER	
9. SPONSORING/MONITORING AGENCY NAME(S) AND ADDRESS(ES) National Aeronautics and Space Administration Langley Research Center Hampton, VA 23681-2199			10. SPONSORING/MONITORING AGENCY REPORT NUMBER NASA/CR-2001-211255	
11. SUPPLEMENTARY NOTES Funding for this work was provided by the Life Cycle Simulation element of the Intelligent Synthesis Environment Program under the task entitled "Structural Acoustic Simulation in Operational Environments." S. A. Rizzi of NASA LaRC was task lead.				
12a. DISTRIBUTION/AVAILABILITY STATEMENT Unclassified-Unlimited Subject Category 71 Distribution: Standard Availability: NASA CASI (301) 621-0390			12b. DISTRIBUTION CODE	
13. ABSTRACT (Maximum 200 words) A location and positioning system was developed and implemented in the anechoic chamber of the Structural Acoustics Loads and Transmission (SALT) facility to accurately determine the coordinates of points in three-dimensional space. Transfer functions were measured between a shaker source at two different panel locations and the vibrational response distributed over the panel surface using a scanning laser vibrometer. The binaural simulation test matrix included test runs for several locations of the measuring microphones, various attitudes of the mannequin, two locations of the shaker excitation and three different shaker inputs including pulse, broadband random, and pseudo-random. Transfer functions, auto spectra and coherence functions were acquired for the pseudo-random excitation. Time histories were acquired for the pulse and broadband random input to the shaker. The tests were repeated with a reflective surface installed. Binary data files were converted to universal format and archived on compact disk.				
14. SUBJECT TERMS Acoustics; Binaural Simulation; Structural Acoustics			15. NUMBER OF PAGES 23	
			16. PRICE CODE A03	
17. SECURITY CLASSIFICATION OF REPORT Unclassified	18. SECURITY CLASSIFICATION OF THIS PAGE Unclassified	19. SECURITY CLASSIFICATION OF ABSTRACT Unclassified	20. LIMITATION OF ABSTRACT UL	